

# Multiple-Access Insights from Bounds on Sensor Localization

Swaroop Venkatesh and R. Michael Buehrer

Mobile and Portable Radio Research Group (MPRG), Virginia Tech, Blacksburg, VA 24061

Email: {vswaroop, buehrer}@vt.edu

## Abstract

*In this paper, we build on known bounds on localization in sensor networks and provide new insights that can be used in multiple-access design from a localization perspective. Specifically, we look at the Cramer-Rao lower bound (CRLB) for the estimation of a sensor's location given unbiased Gaussian range estimates from a set of location-aware "anchor" nodes. A novel characterization of the accuracy of sensor location-estimates is derived, which provides new insights into the design of multiple-access schemes from the perspective of sensor localization accuracy. These insights are validated through the investigation of the performance of a spread-spectrum based multiple-access scheme in an ultra-wideband sensor network.*

## 1. Introduction

The envisioned applications for ad hoc wireless sensor networks often depend on the automatic and accurate location of deployed sensors. In numerous sensor networks, particularly for environmental applications [14] such as water quality monitoring, precision agriculture, and indoor air quality monitoring, the available sensing data may be rendered useless by the absence of accurate sensor location estimates. The availability of accurate sensor location estimates can help reduce configuration requirements and device cost, in addition to providing cross-layer design enhancements. Further, accurate sensor location estimation enables applications such as inventory management, intrusion detection [11], traffic monitoring, and locating emergency workers in buildings [8].

For these applications, accurate and rapid estimation of sensor locations is a critical feature in sensor network design. Consequently, the rate of convergence of sensor location-estimates to the true sensor locations and the temporal characterization of their accuracy is of considerable importance. These problems gain further significance in mobile ad hoc scenarios, such as in the tracking of fire-fighters [8], command-and-control in emergency and battlefield scenarios and the guidance of robots in remote or hazardous locations.

The design of ad hoc "location-aware" sensor networks requires the capability of peer-to-peer range or distance measurement. A sensor whose location is unknown, can estimate its location based on the triangulation of range measurements from location-aware sensors or "anchors", whose locations are known or estimated *a priori*. Range estimates from anchor nodes could be obtained using received signal strength (RSS) or time-of-arrival (TOA) estimation techniques [10].

Ultra-wideband (UWB) is an excellent physical layer solution for location-aware sensor networks due to its robustness in harsh multipath environments, its ability to fuse accurate (on the order of tens of centimeters) ranging with low-data rate communication [10] and its covertness for tactical applications. The narrow pulse duration [2] of UWB signals, and their resistance to multipath fading [21] respectively provide the opportunity for accurate TOA-based and RSS-based range estimation.

Medium-Access Control (MAC) protocol design for sensor networks has typically been investigated from self-organization [15], latency [1] and energy efficiency [22], [7] perspectives. For the applications mentioned previously that are associated with location-aware sensor networks, these design problems need to also be addressed from the perspective of sensor localization. In such applications, localization accuracy may be more significant than metrics such as energy efficiency, e.g., in a fire-fighter tracking network. In this paper, we discuss the problem of MAC design for location-aware UWB sensor networks with respect to the accuracy of sensor location estimates which, to the best of our knowledge, has not been investigated previously.

We first look at the characterization of the accuracy of sensor location estimates through Cramer-Rao lower bound (CRLB) [9] analysis of the problem of location estimation, given unbiased Gaussian range information from location-aware anchors. A novel characterization of the properties of these bounds is presented that allows us to individually assess the impact of different parameters on the accuracy of sensor location estimates. These properties provide insight into the problem of MAC design and indicate that the problem of minimizing localization error in sensor networks is equivalent to the problem of maximizing effective throughput of range information within the network. This obser-

vation is verified by analyzing the performance of a packet-based spread-spectrum multiple access scheme for synchronous UWB sensor networks. The impact of different parameters on the performance of the multiple access scheme is discussed, and bounds on the rate of convergence of location estimates to the true locations are derived. Finally, we discuss the validity of these results when (practical) location estimators that do not attain the Cramer-Rao lower bound are used to compute sensor locations.

This paper is organized as follows: In section 2, we derive the properties of the CRLB for sensor location estimation. These properties serve as a connection to the problem of MAC design for location-aware sensor networks, discussed in section 3. Section 3 also presents the analysis of a spread-spectrum multiple access scheme for UWB-based location-aware sensor networks. An extension of the results to practical estimators, and a discussion of other issues that warrant further investigation, are presented in section 4. We conclude in section 5.

## 2. Cramer-Rao Lower Bound on Localization Accuracy

Let the unknown location of a sensor be  $\mathbf{x} = [x \ y]^T$  (we restrict our attention to the problem of two-dimensional location estimation). The sensor can estimate its location by triangulating the range estimates from anchors with known locations  $\mathbf{x}_i, i = 1, 2, \dots, m$ . These range estimates, obtained via either TOA or RSS-based range estimation, are modeled [13] as unbiased Gaussian estimates:

$$r_i = R_i + n_i, \quad n_i \sim \mathcal{N}(0, \sigma_i^2), \quad i = 1, 2, \dots, m. \quad (1)$$

where  $R_i = \|\mathbf{x} - \mathbf{x}_i\|$  is the true distance between the unlocalized sensor and the  $i$ th anchor and  $\sigma_i^2$  is the variance of the  $i$ th range estimate. In general, the variance  $\sigma_i^2$  of the range estimate [13], [6] increases with  $R_i$ . The term used to quantify the accuracy of sensor's location estimate is called the *localization error* and is defined as:

$$\Omega_{\mathbf{x}} \triangleq E \{ \|\mathbf{x} - \hat{\mathbf{x}}\|^2 \}, \quad (2)$$

where  $\hat{\mathbf{x}}$  represents the estimate of the true sensor location  $\mathbf{x}$ . The CRLB for an unknown parameter  $\theta$  quantifies the performance of the minimum variance unbiased estimator (MVUE) of  $\theta$  [9]. The CRLB for the estimation of a location  $\mathbf{x}$  given  $m$  unbiased Gaussian range estimates  $r_i \sim \mathcal{N}(R_i, \sigma_i^2)$ , from known locations  $\mathbf{x}_i, i = 1, 2, \dots, m$ , in terms of the localization error is given by [13], [4]:

$$\Omega_{\mathbf{x}} = \frac{\sum_{i=1}^m \frac{1}{\sigma_i^2}}{\sum_{i=1}^m \sum_{j=1, j>i}^m \frac{\sin^2(\alpha_i - \alpha_j)}{\sigma_i^2 \sigma_j^2}}, \quad (3)$$

where  $\alpha_i$  is the orientation (angle) of the  $i$ th anchor node relative to the node whose location is being estimated as shown in Figure 1.

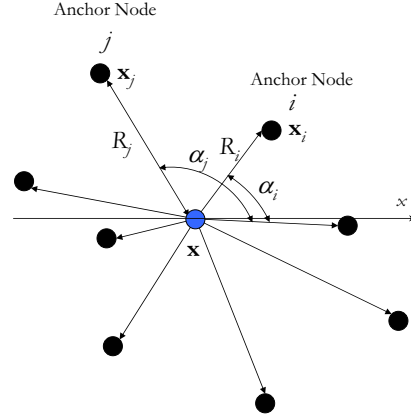


**Figure 1. The problem of sensor location estimation: given range estimates from anchors located at  $\mathbf{x}_i, i = 1, 2, \dots, m$ , the goal is estimate the location  $\mathbf{x}$ .**

From (3), the localization error is a function of (i) the number of range estimates ( $m$ ), (ii) the accuracy (variance) of the range estimates ( $\sigma_i^2, i = 1, 2, \dots, m$ ) and (iii) the geometry of anchor nodes ( $\alpha_i, i = 1, 2, \dots, m$ ). In the following, we derive a novel characterization of the properties of the CRLB that emphasize the individual impact of these parameters on the localization error.

Using the notation

$$\gamma_m \triangleq \sum_{i=1}^m \frac{1}{\sigma_i^2}, \quad \psi_m \triangleq \sum_{i=1}^m \sum_{j=1, j>i}^m \frac{\sin^2(\alpha_i - \alpha_j)}{\sigma_i^2 \sigma_j^2},$$

we define the *generalized Geometric Dilution of Precision* (GGDOP) as

$$\Gamma_m = \frac{\psi_m}{\gamma_m^2} = \frac{\sum_{i=1}^m \sum_{j=1, j>i}^m \frac{\sin^2(\alpha_i - \alpha_j)}{\sigma_i^2 \sigma_j^2}}{\left( \sum_{i=1}^m \frac{1}{\sigma_i^2} \right)^2} \quad (4)$$

This allows the localization error to be expressed as

$$\Omega_{\mathbf{x}} = \frac{\gamma_m}{\psi_m} = \frac{1}{\gamma_m \Gamma_m}. \quad (5)$$

Note that this is a generalized version of the classical GDOP definition [13], [4] which constitutes the case  $\sigma_i^2 = \sigma^2, \forall i$ . However, it must be pointed out that  $\Gamma_m$  is not purely a function of the geometry of anchors relative to the unlocalized sensor, but also depends on the range estimate variances. However, scaling all the range estimate variances by a common factor while maintaining the same relative orientations does not alter the value of  $\Gamma_m$ .

This definition of the GGDOP allows us to isolate the effects of geometry and range variances. For example, from

(5), for a fixed set of range variances, increasing  $\Gamma_m$  decreases the localization error. For a fixed value of  $\Gamma_m$ , if any of the range variances are decreased, the localization error decreases. The following theorem shows that the value of  $\Gamma_m$  is bounded. The proof is provided in Appendix I.

**Theorem 1 (Bounds on GGDOP)** *The minimum and maximum possible values of the GGDOP  $\Gamma_m$  are 0 and  $\frac{1}{4}$  respectively:*

$$0 \leq \Gamma_m \leq \frac{1}{4}.$$

*The maximum value ( $\Gamma_m = \frac{1}{4}$ ) is obtained iff  $\sum_{i=1}^m \frac{\cos 2\alpha_i}{\sigma_i^2} = 0$ ,  $\sum_{i=1}^m \frac{\sin 2\alpha_i}{\sigma_i^2} = 0$ . The minimum value ( $\Gamma_m = 0$ ) is obtained when  $\alpha_i = \alpha$ ,  $\forall i$ .*

**Corollary 2 (Localization Error with Optimal Geometry)** *The localization error in the optimal geometric configuration  $\Gamma_m = \frac{1}{4}$  is given by*

$$\Omega_{\mathbf{x}}^* = \frac{4}{\gamma_m} = \frac{4}{\sum_{i=1}^m \frac{1}{\sigma_i^2}}. \quad (6)$$

From the above theorem, we see that when  $\Gamma_m = 0$ , the anchors are collinear and the localization error  $\Omega_{\mathbf{x}} \rightarrow \infty$ . We further see that in general,  $\Omega_{\mathbf{x}} \geq \frac{4}{\sum_{i=1}^m \frac{1}{\sigma_i^2}}$  (see [4] for a less general result). When  $\sigma_i^2 = \sigma^2$ ,  $\forall i$ , this implies

$$\Omega_{\mathbf{x}}^* = \frac{4\sigma^2}{m}, \quad (7)$$

which suggests that the localization error decreases with increasing  $m$ . Using the above results, the following theorem quantifies the exact dependence of  $\Omega_{\mathbf{x}}$  on the number of range estimates  $m$ . The proof is given in Appendix II.

**Theorem 3 (Dependence on  $m$ )** *Suppose we have an initial geometric configuration of anchor nodes  $\{\alpha_i\}$  with range estimate variances  $\{\sigma_i^2\}$ ,  $i = 1, 2, \dots, m$ . Then the localization error  $\Omega_{\mathbf{x}}(m)$  is given by (3). The introduction of an additional range estimate with variance  $\sigma_{m+1}^2$  from an anchor with orientation  $\alpha_{m+1}$  relative to the unlocalized node, always results in the reduction of the localization error, except when  $\alpha_i = \alpha$ ,  $i = 1, 2, \dots, m+1$ . Specifically,*

$$\Omega_{\mathbf{x}}(m+1) = \frac{\sigma_{m+1}^2 \gamma_m + 1}{\sigma_{m+1}^2 \psi_m + \zeta} \leq \frac{\gamma_m}{\psi_m} = \Omega_{\mathbf{x}}(m),$$

where  $\zeta$  is defined in (18). Equality holds when  $\alpha_1 = \alpha_2 = \dots = \alpha_m = \alpha_{m+1}$ .

**Corollary 4 (Repeated Measurements)** *For the special case:  $\alpha_{m+1} = \alpha_k$ ,  $\sigma_{m+1}^2 = \sigma_k^2$ , where  $k \in \{1, 2, \dots, m\}$ , the improvement in localization error can be viewed as a repeated range measurement followed by averaging of range estimates, which reduces the range variance and the localization error.*

Therefore, except when all the anchor nodes are collinear, increasing the number of range estimates always improves performance. The above theorem indicates that the number of range estimates strongly affects the localization error. This observation serves as a connection to the problem of MAC design for location-aware sensor networks, as we describe in the following section.

### 3. UWB Sensor Localization using Spread-Spectrum Multiple Access

It was demonstrated in the previous section that, for the MVUE [9] of a sensor's location given unbiased Gaussian range information, the number of available range estimates strongly affects the accuracy of the sensor's location estimate. It was shown that, except when all anchors were collinear, increasing the number of range estimates results in the reduction of the localization error. Even when connectivity with anchors is limited, repeated range measurements allow averaging of range estimates, which reduces their variance and, hence, the localization error.

From the perspective of MAC design, it stands to reason that a protocol that allows each unlocalized sensor to accumulate a large number of range estimates in a given duration, increases the likelihood that an accurate estimate of the sensor's location is computed at the end of that duration. Based on this reasoning, as time progresses, a MAC protocol which provides a higher *effective throughput* of range estimates to unlocalized sensors should allow faster convergence of sensor location estimates to the true locations.

In order to verify this conjecture, we investigate the performance of a synchronous spread-spectrum multiple access scheme for UWB Sensor networks. The scheme is based on the assignment of Time-Hopping (TH) codes, that are proposed extensively for UWB communication [20]. The motivation for investigating a scheme based on TH spread-spectrum for UWB sensor networks is due to the following reasons: (1) A spread-spectrum multiple access scheme is a "multi-channel" approach that allows simultaneous transmissions at the cost of incurring multi-access interference (see [18]). This leads to graceful degradation in performance as the number of sensors is increased. (2) Due to significant spreading (transmission-bandwidth to data-rate ratio) inherent in the use of UWB signals for low data-rate applications, "single-channel" collision-avoidance approaches appear wasteful. (3) The covertness of UWB signals makes sensing the channel for collision-avoidance schemes inherently unreliable.

Through the following analysis, we demonstrate that for the modeled UWB sensor network, minimizing the average localization of sensors at any instant of time is equivalent to maximizing the average throughput of the network. We also utilize results from the previous section to derive bounds on the average rate of convergence of sensor location estimates to the true locations. This temporal characterization of lo-

calization accuracy is particularly useful in mobile scenarios.

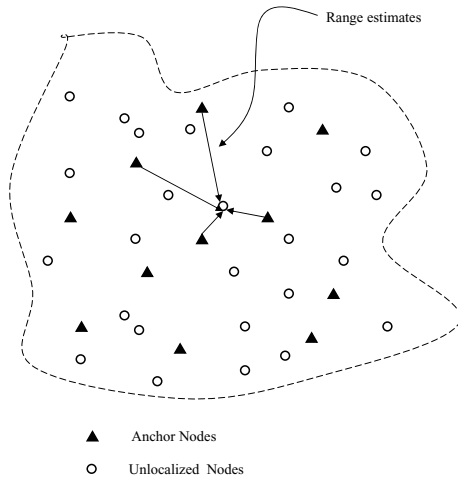


**Figure 2. A sensor network comprising anchor and unlocalized sensors; the anchors transmit packets to the unlocalized sensors. The unlocalized sensors can obtain range estimates using the TOAs of the packets.**

### 3.1. Network Model

A sensor network comprising unlocalized sensors and anchors is illustrated in Figure 2. The following assumptions are made in the modeling of the sensor network:

**Spatial Distribution of Anchors** We assume that the anchor nodes are Poisson distributed over the two-dimensional plane, with an average spatial density  $\Lambda$ . The probability of finding  $k$  nodes in a region with an area  $A$  is given by

$$P\{k \text{ nodes in an area } A\} = e^{-\Lambda A} \frac{(\Lambda A)^k}{k!}. \quad (8)$$

The anchors are assumed to be stationary.

**Packet Transmissions by Anchors** We assume that the time-axis is slotted and that all sensors are synchronized to the slot transitions. Each anchor transmits a single packet at the beginning of a slot with probability  $p$ . The slot width  $T_s$  is assumed to be greater than the packet duration  $T_p$ . The anchor nodes are the “packet-sources” and the unlocalized nodes are the “packet-sinks” of the network. For simplicity, we assume that each packet transmitted by an anchor is intended for a unique unlocalized node. This packet is transmitted on a unique TH spreading-code, specific to an unlocalized node, achieving an effective spreading gain

$N_s$ . This essentially forms multiple TH “code-channels” between pairs of anchors and unlocalized nodes. In general, packets from an anchor node can be broadcast to several unlocalized sensors resulting in multiple packet receptions per packet transmission, but this complicates the analysis considerably (see section 4.2). The transmit power of anchors is assumed to be constant and equal to  $P_T$ .

**TOA-based Range Estimation at unlocalized nodes** An unlocalized sensor that receives a packet from an anchor can estimate the distance  $R$  between them based on the TOA of the packet within the slot, as shown in Figure 3. Since anchor nodes transmit packets at slot-transitions, the TOA of the packet within the slot is proportional to  $R$ . In order to eliminate range ambiguity, we assume  $R \ll cT_s$ , where  $c$  is the speed of light. Since our goal is to model localization accuracy, the contents of the packets are assumed to be the coordinates of the corresponding anchors. From a communications perspective, these packets could contain additional data, since only the TOAs of the packets are used to obtain range estimates.

**Multiple-Access Interference** As several anchor nodes can transmit packets simultaneously at a slot transition, this can result in multiple-access interference (MAI) between simultaneously transmitted packets at unlocalized nodes. We assume that the multiple-access interference seen at an unlocalized node is independent from slot to slot. Further, the interference power is assumed to be constant over the length of a slot.

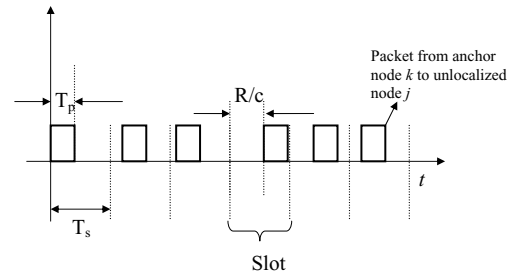


**Figure 3. Slotted Packet Transmissions: based on the delay between a packet’s arrival-time and the previous slot transition, an unlocalized node can estimate the distances to transmitting anchors.**

**Successful reception of packets** A packet is decoded successfully at an unlocalized node if the signal-to-interference-and-noise ratio (SINR)  $\xi$  at the receiver exceeds a threshold  $\xi_T$ , determined by the sensitivity of the

receiver and the strength of coding scheme used. We assume that if the packet is decoded successfully, then a range estimate can be obtained based on its TOA within the slot.

**Traffic and Average Performance** The traffic from anchors to unlocalized sensors is assumed to be balanced, and therefore the analysis of a single unlocalized node represents the generic average over all unlocalized nodes. Coupled with the assumption that the MAI is independent from slot to slot, this allows us to model the average performance by simply looking the behavior of a single “generic” unlocalized sensor over an arbitrary time-slot. Due to the memoryless property of the Poisson distribution [12], without loss of generality, we assume that the generic unlocalized node lies at the origin.

Based on the above assumptions, we first obtain the statistics of the SINR seen at the generic unlocalized node. Using these statistics, we can compute the average effective throughput of packets within the network. This then allows us to characterize the convergence of sensor location estimates to the true sensor locations.

### 3.2. Statistics of the Signal-to-Interference-and-Noise Ratio

The computation of the statistics of the SINR presented here closely follows the analysis presented in [16]. Consider an anchor node  $A$  and an unlocalized node  $B$ . Let the distance between  $A$  and  $B$  be  $R$ . In a given slot, if node  $A$  transmits a packet to node  $B$ , the received signal power [2] can be modeled as

$$P_{r0} = \frac{K_P P_T}{R^\beta}, \quad (9)$$

where  $P_T$  is the transmit power,  $\beta$  is the path-loss exponent in the propagation environment and  $K_P$  is a constant determined by the physical layer. At  $B$ , the received signal power from other interfering anchors that transmit packets in the same slot is given by

$$P_{rk} = \frac{K_P P_T}{r_k^\beta}, \quad k = 1, 2, \dots, \quad (10)$$

where  $r_k$  is the distance between  $B$  and the  $k$ th interferer. The Gaussian model for the MAI in TH-PPM UWB systems was analyzed in [21]. Applying this model to the interference seen at  $B$  from other interfering anchors, the Signal-to-Interference-and-Noise Ratio (SINR)  $\xi$  at  $B$  can be expressed as

$$\xi = \left( \frac{1}{\xi_0} + \frac{K_1}{N_s P_{r0}} \sum_k P_{rk} \right)^{-1},$$

where  $K_1$  is a constant dependent on the receiver structure [21],  $\xi_0$  is the Signal-to-Noise ratio (SNR) and  $P_{rk}$  represents the received power from the  $k$ th interfering anchor.

Using (9) and (10), this can be rewritten as

$$\xi = \left( \frac{1}{\xi_0} + \frac{K_1 R^\beta}{N_s} \sum_k \frac{1}{r_k^\beta} \right)^{-1}. \quad (11)$$

The SINR  $\xi$  is a random variable, since it depends on the spatial locations of the interfering anchor nodes. Since in any slot, the probability that an anchor node is transmitting is  $p$ , the set of interfering anchors form a spatial Poisson process [16] with average density  $\Lambda' = p\Lambda$ . Suppose we define the “effective interference” as the random variable  $Y$ :

$$Y \triangleq \sum_k \frac{1}{r_k^\beta}. \quad (12)$$

Then  $Y$  represents the spatial dependence of the total interference seen from all interfering anchor nodes. Let  $Y_a$  represent the effective interference seen from the interferers located within a disk  $D_a$  of radius  $a$  from  $B$ . The characteristic function of  $Y_a$  is given by

$$\begin{aligned} \phi_{Y_a}(\omega) &= E \{ e^{j\omega Y_a} \} \\ &= E_k \{ E \{ e^{j\omega Y_a} | k \text{ interfering anchors in } D_a \} \} \end{aligned} \quad (13)$$

Given that there are  $k$  interfering anchors in  $D_a$ , and due to the nature of the Poisson process, the distribution of their locations is that of  $k$  independent and identically distributed points with uniform distribution. Their distances from  $B$  are distributed as:

$$f_R(r) = \begin{cases} \frac{2r}{a^2} & r \leq a \\ 0 & \text{otherwise.} \end{cases}$$

Then, it is straightforward to show that

$$E \{ e^{j\omega Y_a} | k \text{ interfering anchors in } D_a \} = \left( \int_0^a \frac{2r}{a^2} e^{\frac{j\omega}{r^\beta}} dr \right)^k.$$

From (8) and (13),

$$\begin{aligned} \phi_{Y_a}(\omega) &= \sum_{k=0}^{\infty} e^{-\Lambda' \pi a^2} \frac{(\Lambda' \pi a^2)^k}{k!} \left( \int_0^a \frac{2r}{a^2} e^{\frac{j\omega}{r^\beta}} dr \right)^k \\ &= \exp \left( \Lambda' \pi a^2 \left( \int_0^a \frac{2r}{a^2} e^{\frac{j\omega}{r^\beta}} dr - 1 \right) \right). \end{aligned}$$

It can be shown that [16] for  $\beta > 2$ , the characteristic function of  $Y$  is obtained by allowing  $a \rightarrow \infty$  in the above expression, which leads to

$$\begin{aligned} \phi_Y(\omega) &= \lim_{a \rightarrow \infty} \phi_{Y_a}(\omega) \\ &= \exp \left( j\Lambda' \pi \omega \left( \int_0^\infty t^{-\frac{2}{\beta}} e^{j\omega t} dt \right) \right) \\ &= \exp \left( -\pi p \Lambda e^{-\frac{\pi}{\beta}} \Gamma \left( 1 - \frac{2}{\beta} \right) \omega^{\frac{2}{\beta}} \right). \end{aligned}$$

This has the form of the characteristic function of a symmetric  $\alpha$ -stable ( $S\alpha S$ ) distribution with a dispersion factor

$\frac{2}{\beta}$ . A closed-form expression for the cumulative distribution function (CDF) associated with the above characteristic function [5] when  $\beta = 4$ , (resulting in the Levy distribution) is known:

$$F_Y(y) = \operatorname{erfc}\left(\frac{\pi^{\frac{3}{2}} p \Lambda}{2\sqrt{y}}\right). \quad (14)$$

### 3.3. Packet Success Probability

For  $\beta = 4$ , from (11) and (14), the probability of the SINR  $\xi$  crossing the threshold  $\xi_T$  is given by

$$\begin{aligned} P_s &= \Pr\{\xi \geq \xi_T\} = F_Y\left(\frac{N_s}{K_1 R^4} \left(\frac{1}{\xi_T} - \frac{1}{\xi_0}\right)\right) \\ &= \operatorname{erfc}\left(\frac{p\pi\Lambda R^2}{\sqrt{\left(\frac{4N_s}{K_1\pi} \left(\frac{1}{\xi_T} - \frac{1}{\xi_0}\right)\right)}}\right). \end{aligned} \quad (15)$$

Since  $\operatorname{erfc}(\cdot)$  is a monotonically decreasing function, we see that the probability of successfully decoding a packet  $P_s$  (i) increases as the spreading gain  $N_s$  increases, and (ii) decreases as the transmission probability  $p$ , the distance  $R$  and the density of anchor nodes  $\Lambda$  increase. It must be noted that although the results here are derived for  $\beta = 4$ , similar trends are observed for values of  $\beta > 2$  via simulation.

Based on this expression, we can now compute the average effective throughput of packets from anchor nodes to unlocalized nodes. In terms of the packets per slot, the effective throughput is simply the probability of successful packet delivery at an unlocalized node. Assuming a uniform local traffic matrix and equal densities of localized and unlocalized nodes, from the analysis provided in [17], the probability of the successful reception of a packet at  $B$  from a given localized node has been shown to be closely approximated by:

$$\begin{aligned} \eta &= (1 - e^{-p}) P_s \\ &= (1 - e^{-p}) \operatorname{erfc}\left(\frac{p\pi\Lambda R^2}{\sqrt{\left(\frac{4N_s}{K_1\pi} \left(\frac{1}{\xi_T} - \frac{1}{\xi_0}\right)\right)}}\right). \end{aligned}$$

Figure 4(a) shows the average throughput  $\eta$  versus the packet transmission probability  $p$  for different values of the spreading gain  $N_s$ . We see that as the spreading gain increases, the average throughput for a given value of  $p$  increases, due to increase in the resistance to MAI. We also see that there is an optimal value of  $p$  for which the average throughput is maximized. This value of  $p$ , denoted by  $p^\dagger$ , can be obtained by setting the partial derivative of  $\eta$  with respect to  $p$  in (16) to zero, and solving for  $p^\dagger$ .

Figure 4(b) shows the average throughput  $\eta$  versus the packet transmission probability  $p$  for different values of the

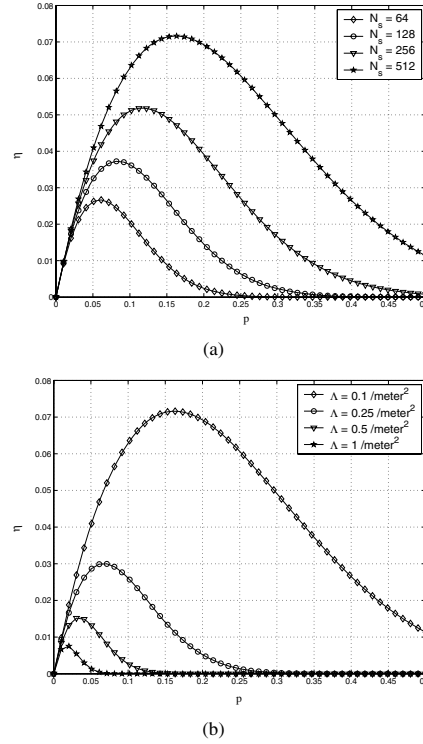


**Figure 4. (a) The average throughput per slot  $\eta$  versus the packet transmission probability  $p$  for different values of the spreading gain  $N_s$ . The values of the other parameters are:  $R = 5$  meters,  $K_1 = 10$ ,  $\xi_T = 10$  dB,  $\xi_0 = 20$  dB,  $\Lambda = 0.1$  meter $^{-2}$ . (b) The average throughput per slot  $\eta$  versus the packet transmission probability  $p$  for different values of the node density  $\Lambda$  with  $N_s = 512$ .**

anchor density  $\Lambda$ . We see that as the anchor density increases, the average throughput for a given value of  $p$  decreases. This is because, for a fixed value of  $p$ , as the anchor node density increases, the average MAI seen at an unlocalized sensor increases.

### 3.4. Convergence of the Localization Error

Since  $\eta$  is the probability that an unlocalized node successfully decodes a packet from a given localized node in a time-slot, it is also the probability that the unlocalized node obtains a range estimate during the slot. Starting at  $t = 0$ , the probability that  $m$  range estimates are accumulated by an unlocalized node by time  $t = nT_s$ , is given by

$$p_m = \binom{n}{m} \eta^m (1 - \eta)^{n-m}.$$

Therefore, the average localization error  $\Omega(t)$  of the unlocalized node at time  $t = nT_s$  is given by

$$\begin{aligned} E\{\Omega(t)\} &= \sum_{m=0}^n p_m \Omega_{\mathbf{x},m} \\ &= \sum_{m=0}^{\infty} \binom{n}{m} \eta^m (1-\eta)^{n-m} \Omega_{\mathbf{x},m}. \end{aligned}$$

Applying the lower bound in (6) for  $\Omega_{\mathbf{x},m}$ , we have

$$E\{\Omega_{\mathbf{x}}(nT_s)\} \geq \sum_{m=0}^n \binom{n}{m} \eta^m (1-\eta)^{n-m} \left( \frac{4}{\gamma m} \right).$$

Assuming equal range variances  $\sigma_i^2 = \sigma_0^2, \forall i$ , we have  $\gamma_m = \frac{m}{\sigma_0^2}$ , we obtain

$$E\{\Omega(nT_s)\} \geq \sum_{m=0}^n \binom{n}{m} \eta^m (1-\eta)^{n-m} \left( \frac{4\sigma_0^2}{m} \right). \quad (16)$$

Figure 5 shows the variation of the average localization error

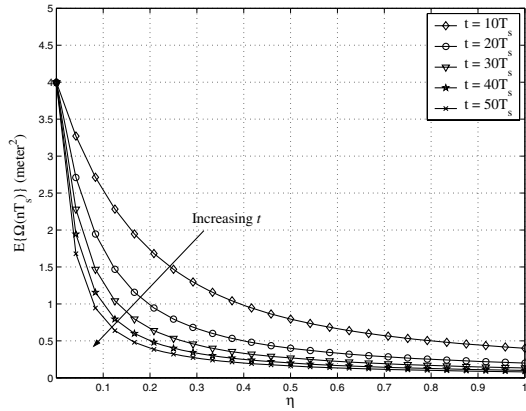


**Figure 5. The average localization error  $E\{\Omega(nT_s)\}$  versus  $\eta$  for different time-instants; The values of the other parameters are:  $R = 5$  meters,  $K_1 = 10$ ,  $\xi_T = 10$  dB,  $\xi_0 = 20$  dB,  $N_s = 256$ ,  $\sigma_0 = 1$  meter.**

ror computed using (16) versus  $\eta$  for different time-instants. As conjectured, we see that as the effective throughput increases, the average localization error at each time-instant decreases. Further, we see that as time progresses, the average localization error decreases due to the accumulation of a larger number of range estimates.

For  $\eta \ll 1$  and  $n \gg 1$ , this reduces to

$$\begin{aligned} E\{\Omega(nT_s)\} &\geq 4\sigma_0^2 \sum_{m=0}^n e^{-\eta n} \left( \frac{(\eta n)^m}{m! m} \right) \\ &\geq 4\sigma_0^2 e^{-\eta n} \sum_{m=0}^n \left( \frac{(\eta n)^m}{(m+1)!} \right) \\ &\approx 4\sigma_0^2 \left( \frac{1 - e^{-\eta n}}{n\eta} \right). \end{aligned}$$

Figure 6(b) shows the average localization error at  $t = 100T_s$  for different values of the transmission probability  $p$ . The most important observation to be made here is that the value of  $p$  that maximizes the average throughput  $\eta$  in Figures 4(a) and 4(b) also minimizes the average localization error. This validates our conjecture that maximizing the average throughput  $\eta$  minimizes the average localization error  $E\{\Omega(t)\}$ , at any instant  $t$ .

Therefore, we have shown that the problem of minimizing the average localization error in the modeled UWB sensor networks is identical to the commonly studied problem of maximizing the throughput of packets within the network. This is intuitive since the accuracy of sensor location estimates was shown to be dependent on the amount of range information available. As range information is available through the TOAs of packets, increasing the rate of transport of this range information over the network should improve sensor localization accuracy.

The results derived in this paper are applicable to any localization system where: (a) the localization accuracy is a monotonically decreasing function of the number of range estimates, and (b) the successful estimation of ranges are contingent on the successful detection of packets.

## 4. Other Issues and Future Work

The CRLB localization error given by (3) provides a benchmark for evaluating the performance of practical location estimators, but does not explicitly describe the estimator that achieves it. In this section, we show that the connection between localization error and throughput observed using the CRLB holds for the practical LS estimator [3], although it does not attain the CRLB. We also briefly described some practical issues and potential avenues for future work in the modeling of location-aware sensor networks.

### 4.1. The Least-Squares (LS) estimator

The Least-Squares (LS) estimation approach is known to be suitable if the PDF of the available data is not known [9]. Denoting the LS estimate of the node's location by  $\hat{\mathbf{x}}_{LS}$ , the localization error for the LS estimator is defined as

$$\Omega_{\mathbf{x},LS} \triangleq E\{\|\mathbf{x} - \hat{\mathbf{x}}_{LS}\|^2\}.$$

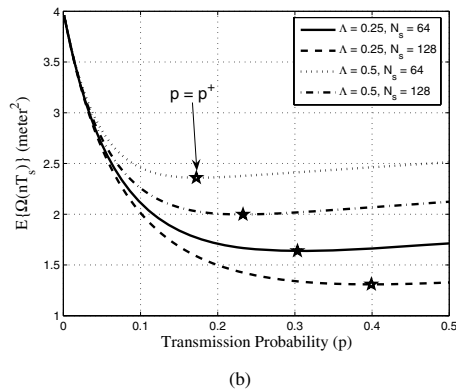
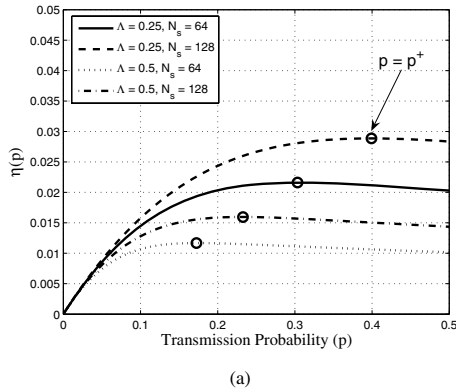


**Figure 6. (a) Lower bound on the average localization error  $E\{\Omega(t)\}$  at  $t = 100T_s$  versus the transmission probability  $p$ . The value of  $\sigma_0 = 0.5$  meters. (b) The effective throughput per slot  $\eta$  versus the transmission probability  $p$ .**

Since the model for the range data is non-linear, the LS estimator [9] is not the MVUE, and consequently does not attain the CRLB. This is also seen in Figure 7, where the performance of the LS estimator is compared with the CRLB in terms of the localization error given unbiased Gaussian range estimates. The details of the simulation are as follows:  $m$  anchor nodes whose locations are known exactly are dispersed randomly over an  $L \times L$  meter<sup>2</sup> area. The range estimates  $r_i$  from these  $m$  are Gaussian random variables with mean  $R_i$  and variance  $\sigma_i^2$  given by  $\sigma_i^2 = K_E R_i^\beta$ . The values of  $K_E$  and  $\beta$  used for this simulation were 0.01 and 2 respectively. We also make another important observation: as shown with the CRLB in Theorem 3, the LS localization error decreases with increasing  $m$ , and therefore the relationship between the localization error and the effective throughput of the sensor network still holds.

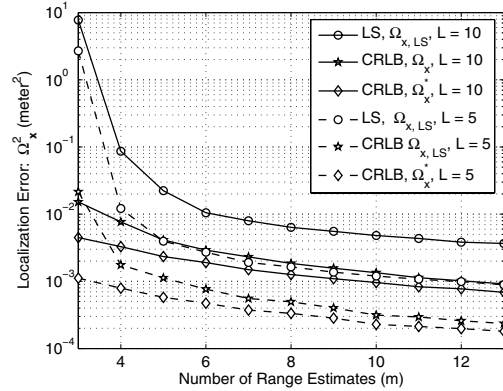


**Figure 7. Comparison of the LS estimator with the CRLB for two-dimensional location estimation given  $m$  unbiased Gaussian range estimates.**

#### 4.2. Realistic modeling of Location-Aware sensor networks from a Localization perspective

In the modeling of the UWB sensor network, several simplifying assumptions were made in an effort to make the analysis simple yet insightful. However, in order to gain a better understanding of the behavior of practical location-aware sensor networks, further investigation is required into more realistic models for such networks from a localization perspective. Below, we list some aspects of the modeling of location-aware sensor networks that warrant investigation and require more sophisticated modeling strategies.

**Synchronization:** In the modeling of the UWB sensor network, we assumed that the sensors were synchronized, which allows us to obtain range estimates based on the TOAs of packets. However, in the absence of network-wide synchronization, ranging needs to be performed using a two-way packet-handshake [10]. This approach allows the nodes to achieve synchronization before ranging can be performed.

**Point-to-Point vs. Broadcasting:** It was assumed that an anchor node transmits packets to a single unlocalized node. In general, packets from an anchor node can be broadcast to several unlocalized sensors resulting in multiple packet receptions per packet transmission, which can expedite sensor localization.

**Transmit Power Control:** The transmit power of anchors is assumed to be constant and equal to  $P_T$ , but in general,

an adaptive power control scheme [19] could be applied, resulting in a larger number of range estimates at unlocalized nodes.

**Transmission Probability:** The transmission probability  $p$  was treated as an independent parameter. However, in a practical scenario, it would be correlated with relative proportions of anchor nodes and unlocalized nodes. For instance, if there are relatively few anchors compared to unlocalized nodes, then the packet transmission probability of the anchors could be much larger than the case where there are fewer unlocalized nodes than anchors. Further, in the presence of mobility, the requirement of frequently updating sensor location-estimates could increase transmission probabilities.

**Node densities** The analysis presented considers a single unlocalized node located at the origin with equal densities of localized and unlocalized nodes. However, in the general case, the densities of localized and unlocalized nodes can be different. Further, these densities can vary with time: the unlocalized nodes that obtain accurate location-estimates can serve as anchors, e.g., after their localization error drops below a certain threshold.

**Node mobility** It was assumed that all nodes, localized and unlocalized, are stationary. This can be extended to the case where the unlocalized nodes are mobile: Range estimates are gathered over a window of time, during which a mobile node is assumed to be stationary, and location estimates are computed at the end of such a “ranging window” [18]. The spatial distributions of nodes can be assumed to vary independently from window to window.

**Range Estimate Variances** The range variances for TOA and RSS based are known to be inversely proportional to the SINR [23], and therefore depend on interference and the distances between nodes. For simplicity in our analysis, we treated the range variances as a constant, and not as a random variable. The throughput  $\eta$  was expressed as a function of the distance between two nodes  $R$ , which in general, should also be treated as a random variable. Further, through the use of the bound derived in (6), we were able to eliminate the dependence on geometry which plays an important role in determining the localization error.

## 5. Conclusions

Some properties of the Cramer-Rao lower bound for sensor location estimation were derived to provide insight into the problem of MAC design. These properties suggested that the problem of minimizing localization error in sensor networks was equivalent to the problem of maximizing effective throughput of range information within the network.

This conjecture was validated by analyzing the performance of spread-spectrum multiple access schemes for synchronous UWB sensor networks. The validity of these results when practical location estimators — that do not attain the Cramer-Rao lower bound — are used, was also verified.

## Appendix I: Bounds on $\Gamma_m$

The generalized GDOP is defined by

$$\begin{aligned}\Gamma_m &= \frac{\psi_m}{\gamma_m^2} = \frac{\sum_{i=1}^m \sum_{j=1, j>i}^m \frac{\sin^2(\alpha_i - \alpha_j)}{\sigma_i^2 \sigma_j^2}}{\left(\sum_{i=1}^m \frac{1}{\sigma_i^2}\right)^2} \\ &= \frac{1}{4} \frac{\left(\sum_{i=1}^m \frac{\cos 2\alpha_i}{\sigma_i^2}\right)^2 + \left(\sum_{i=1}^m \frac{\sin 2\alpha_i}{\sigma_i^2}\right)^2}{4 \left(\sum_{i=1}^m \frac{1}{\sigma_i^2}\right)^2}.\end{aligned}$$

When  $\alpha_i = \alpha_j$ , we see that we obtain the lower bound,  $\Gamma_m = 0$ . The upper limit  $\Gamma_m = \frac{1}{4}$  is achieved when  $\sum_{i=1}^m \frac{\cos 2\alpha_i}{\sigma_i^2} = 0$  and  $\sum_{i=1}^m \frac{\sin 2\alpha_i}{\sigma_i^2} = 0$ . A specific case of the above result is discussed in [4].

## Appendix II

Given  $m$  unbiased Gaussian range estimates, the localization error is given by:

$$\Omega_x(m) = \frac{\sum_{i=1}^m \frac{1}{\sigma_i^2}}{\sum_{i=1}^m \sum_{j=1, j>i}^m \frac{\sin^2(\alpha_i - \alpha_j)}{\sigma_i^2 \sigma_j^2}} = \frac{\gamma_m}{\psi_m}$$

We would like to analyze the effect of adding a new node with parameters  $(\alpha_{m+1}, \sigma_{m+1}^2)$ :

$$\begin{aligned}\Omega_x(m+1) &= \frac{\sum_{i=1}^{m+1} \frac{1}{\sigma_i^2}}{\sum_{i=1}^{m+1} \sum_{j=1, j>i}^{m+1} \frac{\sin^2(\alpha_i - \alpha_j)}{\sigma_i^2 \sigma_j^2}} \\ &= \frac{\gamma_m + \frac{1}{\sigma_{m+1}^2}}{\psi_m + \frac{1}{\sigma_{m+1}^2} \sum_{i=1}^m \frac{\sin^2(\alpha_i - \alpha_{m+1})}{\sigma_i^2}} \\ &= \frac{\sigma_{m+1}^2 \gamma_m + 1}{\sigma_{m+1}^2 \psi_m + \zeta}\end{aligned}\quad (17)$$

where we define

$$\zeta \triangleq \sum_{i=1}^m \frac{\sin^2(\alpha_i - \alpha_{m+1})}{\sigma_i^2}.\quad (18)$$

Defining the angle  $\nu$  as

$$\nu = \frac{1}{2} \arctan \frac{\sum_{i=1}^m \frac{\sin 2\alpha_i}{\sigma_i^2}}{\sum_{i=1}^m \frac{\cos 2\alpha_i}{\sigma_i^2}},\quad (19)$$

after some simplification, we can show that

$$\zeta = \frac{\gamma_m}{2} - \frac{\sqrt{\gamma_m^2 - 4\psi_m} \cos(2\alpha_{m+1} - 2\nu)}{2}\quad (20)$$

From (17) and (20),

$$\Omega_{\mathbf{x}}(m+1) = \frac{\sigma_{m+1}^2 \gamma_m + 1}{\sigma_{m+1}^2 \psi_m + \frac{\gamma_m - \sqrt{\gamma_m^2 - 4\psi_m} \cos(2\alpha_{m+1} - 2\nu)}{2}}$$

In order to compute the change in the localization error due to the addition of a new node, we look at

$$\begin{aligned} & \Omega_{\mathbf{x}}(m) - \Omega_{\mathbf{x}}(m+1) \\ &= \frac{\gamma_m}{\psi_m} - \frac{\sigma_{m+1}^2 \gamma_m + 1}{\sigma_{m+1}^2 \psi_m + \frac{\gamma_m - \sqrt{\gamma_m^2 - 4\psi_m} \cos(2\alpha_{m+1} - 2\nu)}{2}} \\ &= \frac{\frac{\gamma_m}{2} - \frac{\gamma_m \sqrt{\gamma_m^2 - 4\psi_m} \cos(2\alpha_{m+1} - 2\nu)}{2} - \psi_m}{\psi_m \left( \sigma_{m+1}^2 \psi_m + \frac{\gamma_m}{2} - \frac{\sqrt{\gamma_m^2 - 4\psi_m} \cos(2\alpha_{m+1} - 2\nu)}{2} \right)} \\ &= \frac{\frac{1}{2} - \frac{\sqrt{1-4\Gamma_m} \cos(2\alpha_{m+1} - 2\nu)}{2} - \Gamma_m}{\Gamma_m \left( \sigma_{m+1}^2 \psi_m + \frac{\gamma_m}{2} - \frac{\sqrt{\gamma_m^2 - 4\psi_m} \cos(2\alpha_{m+1} - 2\nu)}{2} \right)} \end{aligned}$$

Since the denominator is always positive, to verify whether there is an improvement in the location error or not, we verify that:

$$\begin{aligned} & \frac{1}{2} - \frac{\sqrt{1-4\Gamma_m} \cos(2\alpha_{m+1} - 2\nu)}{2} - \Gamma_m \\ &= \frac{(\sqrt{1-4\Gamma_m} - \cos(2\alpha_{m+1} - 2\nu))^2 + \sin^2(2\alpha_{m+1} - 2\nu)}{2} \geq 0 \end{aligned}$$

where equality holds when  $\Gamma_m = 0$  and  $\alpha_{m+1} = \nu$ . This holds when  $\alpha_i = \alpha$ ,  $i = 1, 2, \dots, m+1$ .

## References

- [1] I. F. Akyildiz, W. Su, Y. Sankarasubramaniam, and E. Cayirci. A survey on sensor networks. In *IEEE Communications Magazine*, volume 40, pages 102–114, August 2002.
- [2] R. Buehrer, W. Davis, A. Safaai-Jazi, and D. Sweeney. Ultra-wideband propagation measurements and modeling - darpa netex final report. Technical report, January 2004. available at [http://www.mprg.org/people/buehrer/ultra/darpa\\_netex.shtml](http://www.mprg.org/people/buehrer/ultra/darpa_netex.shtml).
- [3] J. J. Caffery. A new approach to the geometry of TOA location. In *2000 IEEE Vehicular Technology Conference*, volume 4, pages 1943 – 1949, September 2000.
- [4] C. Chang and A. Sahai. Estimation bounds for localization. In *IEEE SECON 2004*, pages 415 – 424, 4-7 Oct. 2004.
- [5] W. Feller. *A Introduction to Probability Theory and its Applications*. 1966. Vol. II, Wiley.
- [6] S. Gezici, Z. Tian, G. B. Giannakis, H. Kobayashi, A. F. Molisch, H. V. Poor, and Z. Sahinoglu. Localization via ultra-wideband radios. In *IEEE Signal Processing Magazine*, volume 22, pages 70– 84, July 2005.
- [7] C. Guo, L. C. Zhong, and J. M. Rabaey. Low power distributed MAC for ad hoc sensor radio networks. In *2001 IEEE Global Telecommunications Conference (GLOBE-COM '01)*, volume 5, pages 2944 – 2948, November 2001.
- [8] S. J. Ingram, D. Harmer, and M. Quinlan. Ultra-wideband Indoor Positioning Systems and their Use in Emergencies. In *Position Location and Navigation Symposium, 2004. PLANS 2004*, Rome, Italy, April 2004.
- [9] S. M. Kay. *Fundamentals of Statistical Processing, Volume I: Estimation Theory*. 1993. 2nd Edition, Prentice-Hall Inc.
- [10] J.-Y. Lee and R. A. Scholtz. Ranging in a dense multipath environment using an UWB radio link. In *IEEE Journal on Selected Areas in Communications*, volume 20, pages 1677–1683, December 2002.
- [11] R. L. Moses, D. Krishnamurthy, and R. Patterson. An auto-calibration method for unattended ground sensors. In *ICASSP 2002*, pages 2941–2944, May 2002.
- [12] A. Papoulis. *Probability, Random Variables and Stochastic Processes*. 1991. 3rd Edition, McGraw-Hill Inc.
- [13] N. Patwari, A. O. Hero, M. Perkins, N. S. Correal, and R. J. O’Dea. Relative location estimation in wireless sensor networks. In *IEEE Transactions on Signal Processing*, volume 51, pages 2137–2148, Aug. 2003.
- [14] J. M. Rabaey, M. J. Ammer, J. L. da Silva, D. Patel, and S. Roundy. Picoradio supports ad hoc ultra-low power wireless networking. In *IEEE Comput.*, volume 33, pages 42–48, July 2000.
- [15] K. Sohrabi, J. Gao, V. Ailawadhi, and G. J. Pottie. Protocols for self-organization of a wireless sensor network. In *IEEE Personal Communications*, volume 7, pages 16–27, October 2000.
- [16] E. Sousa and J. A. Silvester. Optimum transmission ranges in a direct-sequence spread-spectrum multihop packet radio network. In *IEEE Journal on Selected Areas in Communications*, volume 8, pages 762–771, June 1990.
- [17] E. S. Sousa and J. A. Silvester. Spreading code protocols for distributed spread-spectrum packet radio networks. In *IEEE Transactions on Communications*, volume 36, pages 272–281, February 1988.
- [18] S. Venkatesh and R. M. Buehrer. Multiple-access design in UWB Position Location Networks. In *2006 Proceedings of the IEEE Conference on Wireless Communications and Networking (WCNC 2006)*, April 3-6 2006.
- [19] S. Venkatesh and R. M. Buehrer. Power-Control in UWB Position Location Networks. In *2006 Proceedings of the IEEE Conference on Communications (ICC 2006)*, June 11th-15th 2006.
- [20] M. Z. Win and R. A. Scholtz. Impulse radio: How it works. In *IEEE Communications Letters*, volume 2, pages 36–38, February 1998.
- [21] M. Z. Win and R. A. Scholtz. Ultra-Wide Bandwidth Time-Hopping Spread-Spectrum Impulse Radio for Wireless Multiple-Access Communications. In *IEEE Transactions on Communications*, volume 48, April 2000.
- [22] W. Ye, J. Heidemann, and D. Estrin. An energy-efficient MAC protocol for wireless sensor networks. In *Proceedings of INFOCOM 2002*, pages 1567 – 1576, June 2002.
- [23] J. Zhang, R. R. A. Kennedy, and T. D. Abhayapala. Cramer-Rao lower bounds for the time delay estimation of UWB signals. In *2004 IEEE International Conference on Communications*, pages 3424 – 3428 vol.6, 20-24 June 2004.